

Quantum phase transitions, frustration and the Fermi surface in the Kondo lattice model

Eitan Eidelstein, S. Moukouri and Avraham Schiller

Racah Institute of Physics, The Hebrew University, Jerusalem 91904, Israel

The quantum phase transition from a spin-Peierls phase with a small Fermi surface to a paramagnetic Luttinger-liquid phase with a large Fermi surface is studied in the framework of a one-dimensional Kondo-Heisenberg model that consists of an electron gas away from half filling, coupled to a spin-1/2 chain by Kondo interactions. The Kondo spins are further coupled to each other with isotropic nearest-neighbor and next-nearest-neighbor antiferromagnetic Heisenberg interactions which are tuned to the Majumdar-Ghosh point. Focusing on three-eighths filling and using the density-matrix renormalization-group (DMRG) method, we show that the zero-temperature transition between the phases with small and large Fermi momenta appears continuous, and involves a new intermediate phase where the Fermi surface is not well defined. The intermediate phase is spin gapped and has Kondo-spin correlations that show incommensurate modulations. Our results appear incompatible with the local picture for the quantum phase transition in heavy fermion compounds, which predicts an abrupt change in the size of the Fermi momentum.

PACS numbers: 75.30.Mb, 71.10.Hf, 71.10.pm, 71.27.+a

I. INTRODUCTION

The Kondo lattice model (KLM) was historically introduced to describe the competition between singlet formation and magnetic ordering in heavy fermion systems.¹ In heavy fermion materials, localized f -shell electrons hybridize with itinerant electrons. Depending on whether the f electrons participate in the formation of the Fermi surface (FS) or not, the latter may be large or small.² The Fermi momentum k_F^L is large in the sense that the FS encloses a volume that counts both the number of conduction electrons and local moments.^{2,3} This is in contrast to a small Fermi momentum k_F^S , whose FS encloses a volume that counts the number of conduction electrons only.

An earlier issue debated on the KLM was whether the formation of a large FS is consistent with Luttinger's theorem.⁴ In other terms, the question was whether the KLM can account for a large FS given that the f electrons are represented by their spin degrees of freedom only. Investigations of the one-dimensional (1D) KLM through numerical⁵⁻⁹ and analytical^{3,10} approaches have yielded rather consistent evidence for a ground state with a large FS in the paramagnetic regions of the model. Yet recent numerical calculations have suggested the existence of a second phase where the FS is small.¹¹ Such a phase will necessarily have a broken-symmetry ground state, otherwise it would be inconsistent with Luttinger's theorem.^{3,10} For reviews on the 1D KLM, we refer the reader to Refs. 5 and 12.

In the last decade, the question of the size of the FS in the KLM has gained renewed interest in connection with quantum criticality and the related non-Fermi-liquid phases of heavy fermion materials. The local picture for the quantum phase transition (QPT) in these compounds predicts that the size of the FS would change abruptly at the quantum critical point.^{13,14} The com-

posite quasiparticles forming the large FS are projected to breakdown as the system is driven across the critical point, leaving behind a small Fermi volume that counts the number of conduction electrons only. It is still unclear how such a sudden change of the FS is consistent with a second-order phase transition.

One-dimensional models, for which powerful methods of solution are available, are currently the primary tool for gaining reliable information about QPT in the KLM. However, magnetic orderings that break spin-rotational symmetry are prohibited in 1D. Hence, it is necessary to study the QPT between the paramagnetic phase with a large FS and alternative phases of the Ising or spin-Peierls type.¹⁵ If the f electrons are in an Ising or a dimerized phase, they would remain decoupled from the conduction electrons at low energies also in the presence of a sufficiently small Kondo coupling as compared to the gap. Consequently, the FS would be small. A QPT toward a ground state with a large FS would occur upon increasing the Kondo coupling. This latter phase is presumably a Luttinger liquid (LL) or a spin-gapped phase.

In this paper, we study the evolution of the ground state of a 1D KLM from a spin-Peierls phase with a small Fermi momentum k_F^S to a LL phase with a large Fermi momentum k_F^L . To this end, we augment the conventional KLM with isotropic nearest-neighbor and next-nearest-neighbor spin-exchange interactions among the Kondo spins, and tune them to the Majumdar-Ghosh point.¹⁶ The inclusion of next-nearest-neighbor coupling is a crucial ingredient of our study, as it supports a broken-symmetry ground state with a small FS for small Kondo couplings.

Focusing on three-eighths filling and using the density-matrix renormalization group method (DMRG),¹⁷ we find a zero-temperature transition that is more complex than the predictions of the local critical theory. In particular, we identify an intermediate spin-gapped phase in between the spin-Peierls and LL phases where

the Fermi momentum cannot be defined. Instead, the electron momentum distribution function $n(k)$ displays a shallow peak at a new characteristic momentum k^* that lies in between k_F^S and k_F^L , and which shifts toward k_F^L on going from the spin-Peierls to the LL phase. Concomitantly, there is a maximum at $2k^*$ in the magnetic structure factor $S(k)$ of the Kondo spins. We show that this behavior can be understood as a consequence of the magnetic frustration induced by competing spin-exchange couplings generated by the Ruderman-Kittel-Kasuya-Yosida (RKKY) interaction. In contrast to $n(k)$ and $S(k)$, neither the Fourier transform of the local conduction-electron density $n_r(k)$ nor the density-density correlation function $C(k)$ show any special signatures related to k^* . Rather, the transition from the spin-Peierls to the spin-gapped phase is manifest in $C(k)$ by the smearing of a cusp at $2k_F^S$ and the emergence of a peak at $2k_F^L$. Our results appear incompatible with the local picture for the QPT in heavy fermion compounds.

The remainder of the paper is organized as follows. In Sec. II we present the KLM under study, along with details of our DMRG code. A comprehensive set of results for the dimer order parameter, the spin velocity, the electron momentum-distribution function, the magnetic structure factor of the Kondo spins, and various density correlations are described and analyzed in Sec. III. We conclude in Sec. IV with a discussion of the resulting phase diagram and its relevance to heavy fermion compounds.

II. THE MODEL

In this paper we study the following KLM

$$H = -t \sum_{i=1, \sigma}^{L-1} \left\{ c_{i, \sigma}^\dagger c_{i+1, \sigma} + \text{H.c.} \right\} + J_K \sum_{i=1}^L \vec{S}_i \cdot \vec{\tau}_i \\ + J_{H_1} \sum_{i=1}^{L-1} \vec{S}_i \cdot \vec{S}_{i+1} + J_{H_2} \sum_{i=1}^{L-2} \vec{S}_i \cdot \vec{S}_{i+2}, \quad (1)$$

describing a 1D tight-binding conduction band with the hopping term t , interacting via an on-site spin-exchange (Kondo) interaction J_K with an array of localized spins. Here, $c_{i, \sigma}^\dagger$ creates a conduction electron with spin-projection σ at site i , \vec{S}_i represents the localized spin at site i , and $\vec{\tau}_i = \frac{1}{2} \sum_{\sigma, \sigma'} c_{i, \sigma}^\dagger c_{i, \sigma'} (\vec{\sigma})_{\sigma, \sigma'}$ is the conduction-electron spin density at that site. The conduction electrons and spins reside on an L -site lattice with open boundary conditions (OBC). In addition to the Kondo interaction, the localized spins interact among themselves via the nearest-neighbor and next-nearest-neighbor Heisenberg spin-exchange terms J_{H_1} and J_{H_2} , respectively. To avoid the onset of ferromagnetism⁸ we set $J_{H_1} = t/2$, while $J_{H_2} = J_{H_1}/2$ is tuned to the well-known Majumdar-Ghosh point,¹⁶ whose corresponding ground state of the decoupled spin chain is a perfect dimerized state (for even L).

As emphasized above, the inclusion of $J_{H_2} = J_{H_1}/2 > 0$ is a crucial difference from previous DMRG studies of the KLM.^{6-9, 11, 18-20} This additional frustration opens a gap in the spectrum of the isolated spin chain,²¹ enabling the study of the transition from the broken-symmetry dimerized phase with a small FS to the LL phase with a large FS. From a technical standpoint, the dimerization gap significantly reduces the numerical effort that is needed to obtain reliable results as compared to the case where $J_{H_1} = J_{H_2} = 0$,¹⁸⁻²⁰ due to the short-range spin-spin correlations that develop.

We computed the ground state of the Hamiltonian of Eq. (1) using the DMRG method with OBC. We retained between 256 and 512 states in the two external blocks, keeping track of the total number of electrons and the z component of the total spin projection S_z as good quantum numbers. The maximal truncation error was in the order of 10^{-4} when 256 states were kept and in the order of 10^{-5} when 512 states were kept. We studied different lattice sizes up to $L = 64$ sites with J_K varied in the range $0 \leq J_K/t \leq 16$. For concreteness we set the conduction-electron filling equal to $n = 0.75$, which is close to but off half filling, and is rather convenient to tackle numerically. We briefly comment on other filling factors at the end of the paper. All results presented below are restricted to zero temperature. The lattice size is $L = 64$ unless stated otherwise.

III. RESULTS

It is instructive to consider first the limits of small and large J_K , where different phases are expected. When $J_K = 0$, the conduction electrons and spins are decoupled, forming independent chains. The spin chain, being tuned to the dimerized Majumdar-Ghosh phase, is gapped due to the breaking of translational symmetry. The electron chain is gapless in both the spin and charge sectors, as is the overall system. Due to the gap in the spectrum of the isolated spin chain, the Majumdar-Ghosh phase is expected to be stable against the inclusion of a small J_K .

In the opposite limit $J_K \gg t, J_{H_1}$, the conduction electrons and spins bind to form localized singlets. At temperatures below J_K there is no thermal energy to break the Kondo singlets, which can be viewed as holes in the underlying Kondo spin texture. Hence, by analogy with the case where $J_{H_2} = 0$,⁹ the system is described by the $t - J_1 - J_2$ model for holes, with $t \rightarrow t/2$, $J_1 = J_{H_1}$, and $J_2 = J_{H_2}$. Note that the original electronic filling factor n (assumed to be smaller than 1) is converted by this mapping to the hole filling factor $n_{\text{hole}} = n$.²² The corresponding ground state of the $t - J_1 - J_2$ model is expected to be a paramagnetic LL for $n_{\text{hole}} = 0.75$, which differs in symmetry from the dimerized phase at small J_K . Thus, a QPT should occur upon increasing J_K . Below we confirm this scenario and thoroughly discuss the nature of the phase transition.

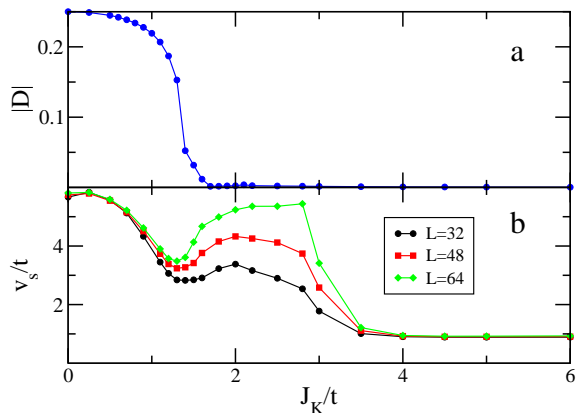


FIG. 1: (Color online) (a) The dimer order parameter $|D|$ of Eq. (2), plotted as a function of J_K/t for $n = 0.75$ and zero temperature. For $J_K = 0$, the system is in a perfect dimer state, corresponding to $|D| = 0.25$. As the Kondo interaction J_K is switched on the dimerization progressively decays until it vanishes for $J_K/t \gtrsim 1.7$. Note the particularly sharp slope around $J_K/t = 1.3$ – 1.4 . (b) The spin velocity v_s of Eq. (3) as a function of J_K/t , plotted for different lattice sizes L and $n = 0.75$. Different qualitative behaviors are observed for weak, intermediate, and strong couplings. In particular, a spin gap opens in the intermediate-coupling regime $1.3 \lesssim J_K/t \lesssim 4$.

A. Dimer order parameter

The first quantity we study is the dimerization order parameter D , defined as

$$D = \frac{2}{3L} \sum_{i=1}^{L-1} \langle \vec{S}_i \cdot \vec{S}_{i+1} \rangle (-1)^i. \quad (2)$$

Here the alternating $(-1)^i$ factor comes to distinguish the dimerized phase from a translational-invariant state. Figure 1(a) depicts the evolution of $|D|$ with increasing J_K . For $J_K = 0$ there is perfect dimerization, corresponding to $|D| = 0.25$. This value of $|D|$ stems from the fact that each spin \vec{S}_i forms a perfect singlet with one of its neighbors and is uncorrelated with its other neighbor. Consequently, $\langle \vec{S}_i \cdot \vec{S}_{i+1} \rangle$ equals $-3/4$ (0) for odd (even) i . With increasing $J_K > 0$, the dimerization order parameter decreases first gradually and then sharply around $J_K/t = 1.3$ – 1.4 . The sharp slope in the latter regime suggests a rather rapid change in the nature of the ground state. Eventually $|D|$ vanishes above $J_K/t \approx 1.7$, indicating the loss of any remnant of the dimer state that forms at small J_K . It should be noted that D shows no significant size dependence due to the short-range spin-spin correlations that are involved.

B. Spin velocity

When $J_K/t \gtrsim 1.7$ translational symmetry is restored, as signaled by the vanishing of D . In order to better

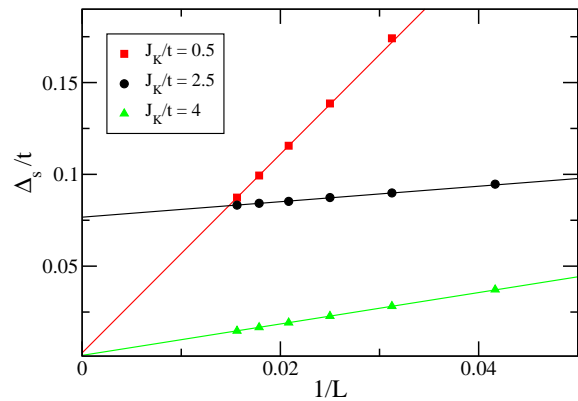


FIG. 2: (Color online) The spin gap $\Delta_s(L)$ as a function of $1/L$, plotted for $n = 0.75$ and $J_K/t = 0.5, 2.5$, and 4 . The solid lines are linear extrapolations to $L \rightarrow \infty$. In contrast to $J_K/t = 0.5$ and 4 , where $\Delta_s(L)$ extrapolates to zero, a finite spin gap $\Delta_s(L \rightarrow \infty) \simeq 0.077t$ is found for $J_K/t = 2.5$.²³

understand the nature of this new phase we computed the spin velocity v_s , defined as

$$v_s(L) = \Delta_s(L)L. \quad (3)$$

Here $\Delta_s(L)$ is the elementary singlet-triplet excitation energy for a system of size L . Figure 1(b) shows $v_s(L)$ for different lattice sizes as a function of J_K . When $J_K/t \lesssim 1.3$, $v_s(L)$ strongly depends on J_K , reflecting the progressive formation of a composite quasiparticle made up of the local spins and the itinerant electrons. By contrast, $v_s(L)$ is almost independent of both J_K and L when $4 \lesssim J_K/t$. This behavior can be understood from the fact that the system is rather well described in this regime by the $t - J_1 - J_2$ model discussed above, which forms a LL when $n_{\text{hole}} = 0.75$. In the intermediate range, $1.3 \lesssim J_K/t \lesssim 4$, $v_s(L)$ depends strongly on both J_K and L , indicating the emergence of a nonzero spin gap Δ_s for $L \rightarrow \infty$.

To support this interpretation we have plotted $\Delta_s(L)$ vs. L in Fig. 2, for three representative values of J_K/t . For both small and large J_K (represented by $J_K/t = 0.5$ and 4 , respectively), $\Delta_s(L)$ extrapolates nicely to zero as $L \rightarrow \infty$, indicative of a gapless state. However, for the intermediate value of $J_K/t = 2.5$, $\Delta_s(L)$ extrapolates to the finite spin gap $\Delta_s/t \approx 0.077$ as $L \rightarrow \infty$.²³ Such a global spin gap is neither consistent with a spin-dimerized phase nor with a LL phase. A similar spin gap was found throughout the range $1.3 \lesssim J_K/t \lesssim 4$, though the precise boundaries of this new phase are somewhat difficult to pin down.²⁴

C. Electron momentum-distribution function

Next we address the size of the FS and its evolution upon going from $J_K = 0$ to $J_K/t = 16$, thereby crossing the three different regimes of small, intermediate and

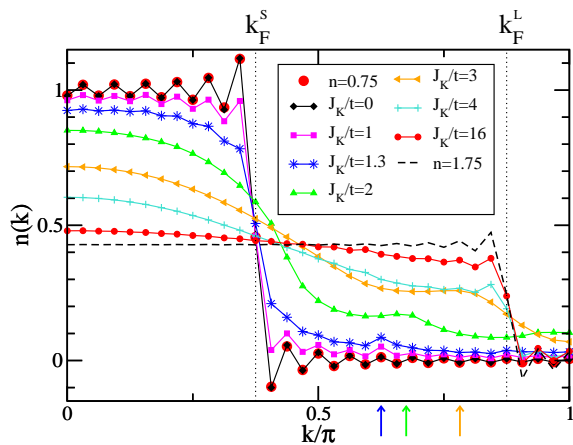


FIG. 3: (Color online) The electron momentum-distribution function of Eq. (4), for $n = 0.75$ and different Kondo couplings $J_K/t = 0, 1, 1.3, 2, 3, 4$ and 16 . When $J_K = 0$, the conduction electrons form a free band, whose exact momentum-distribution function is depicted by the red dots. Accordingly, there is a sharp step in the momentum-distribution function at the (small) Fermi momentum $k_F^S = \pi n/2 = 0.375\pi$. The step at k_F^S persists for small Kondo interactions, $J_K/t \lesssim 1.3$. In the opposite limit of large J_K (represented by $J_K/t = 16$), there is a new step at the large Fermi momentum $k_F^L = \pi(n+1)/2 = 0.875\pi$. The corresponding momentum-distribution function compares rather well with that of a noninteracting tight-binding chain of equal length and the filling $n' = 1 + n = 1.75$, scaled down by a factor of $n/n' = 3/7$ (black dashed line). In contrast to the limits of small and large J_K , there is no clear sign of a FS for the intermediate couplings $J_K/t = 2$ and 3 .

large J_K signaled by D and v_s in Figs. 1 and 2. As pointed out earlier in the introduction, previous computations⁸ on the KLM with $J_{H_2} = 0$ concluded that a large FS forms in the absence of symmetry breaking. Due to the gap in the spectrum of the dimerized Majumdar-Ghosh phase, the conduction electrons and spins remain decoupled at low energies even in the presence of a small J_K , thus forming a small FS. On the other hand, a large FS should be recovered when $J_K \gg t, J_{H_1}$, as the resulting behavior should basically reproduce that of $J_{H_2} = 0$.

In order to study the transition between these vastly different Fermi momenta, we computed the electron momentum-distribution function, defined as

$$n(k) = \sum_{i=1}^L \sum_{\sigma} \langle c_{i,\sigma}^{\dagger} c_{L/2,\sigma} \rangle \cos[k(i - L/2)]. \quad (4)$$

This definition of $n(k)$ differs from the conventional one $n(k) = \sum_{\sigma} \langle c_{k,\sigma}^{\dagger} c_{k,\sigma} \rangle$ due to the OBC used. Nevertheless, it contains similar information on the FS, as we show below. In particular, the two definitions must coincide in the thermodynamic limit $L \rightarrow \infty$, provided that translational symmetry is not broken. To see this we note that the correlator $\langle c_{i,\sigma}^{\dagger} c_{L/2,\sigma} \rangle$ with fixed $i - L/2$ becomes independent of the boundary conditions for $L \rightarrow \infty$.

Converting to periodic boundary conditions and in the presence of translational invariance, Eq. (4) reduces then to $\frac{1}{2} \sum_{\sigma} [\langle c_{k,\sigma}^{\dagger} c_{k,\sigma} \rangle + \langle c_{-k,\sigma}^{\dagger} c_{-k,\sigma} \rangle]$, which is nothing but the conventional momentum-distribution function. Here we made use of the fact that $\langle c_{k,\sigma}^{\dagger} c_{k,\sigma} \rangle$ and $\langle c_{-k,\sigma}^{\dagger} c_{-k,\sigma} \rangle$ are identical by virtue of inversion symmetry.

Figure 3 shows $n(k)$ for different Kondo interactions at the fixed filling factor $n = 0.75$. For $J_K = 0$, one can compute $n(k)$ exactly from the single-particle eigenstates of the decoupled conduction-electron chain. The exact results, depicted by the red circles, essentially coincide with our DMRG data, serving as a critical check for the accuracy of our code. As expected, there is a sharp step in $n(k)$ at the small Fermi momentum $k_F^S = \pi n/2 = 0.375\pi$ of the free band. Note that $n(k)$ oscillates as a function of k , and can become both negative and may exceed one. These finite-size effects are eliminated in the thermodynamic limit $L \rightarrow \infty$. We emphasize, however, that the definition of Eq. (4) does not require that $0 \leq n(k) \leq 1$.

As soon as the Kondo interaction is switched on, the system gradually loses the sharpness of the FS, as expected of an interacting 1D system. Nevertheless, a clear Fermi momentum can still be observed at k_F^S for $J_K/t \lesssim 1.3$, i.e., in the range where a sizeable dimerized order persists (see Fig. 1). In the strong-coupling limit $4 \lesssim J_K/t$ (note that $4t$ is the free conduction-electron band-width), a new well-defined Fermi momentum appears, this time at $k_F^L = \pi(n+1)/2 = 0.875\pi$. This value of k_F corresponds to a FS which encloses a volume that counts both the number of conduction electrons (filling factor of $n = 0.75$) and the number of local moments (“filling factor” of $n = 1$). For comparison, the black dashed line represents the exact momentum-distribution function for a noninteracting tight-binding chain of equal length and the filling $n' = 1 + n = 1.75$, scaled down by a factor of $n/n' = 3/7$. This latter renormalization reflects the fact that the actual conduction-electron filling in our system [corresponding to the integrated weight of $n(k)$] is n rather than $n' = 1 + n$. The agreement is quite surprising.

In contrast to the weak- and strong-coupling regimes, there is no well-defined Fermi momentum for the intermediate couplings $J_K/t = 2$ and 3 . Instead, the sharp structure at k_F^S is rapidly smoothed and suppressed, and a new feature appears at a characteristic momentum k^* located in between k_F^S and k_F^L . This new feature, whose position is marked by the arrows in Fig. 3, first appears for $J_K/t = 1.3$ as a small and shallow peak at $k^* = 0.625\pi$. It continuously shifts toward k_F^L upon increasing J_K , until it coincides with the new Fermi momentum k_F^L for $J_K/t = 4$. As seen from the Friedel oscillations and the density-density correlation function presented below, k^* is not associated with a new Fermi momentum. Rather, it reflects the spin-spin correlations that develop in this range due to the combination of J_{H_1} , J_{H_2} , and the RKKY interaction mediated by the conduction electrons. In other words, k^* stems from the back

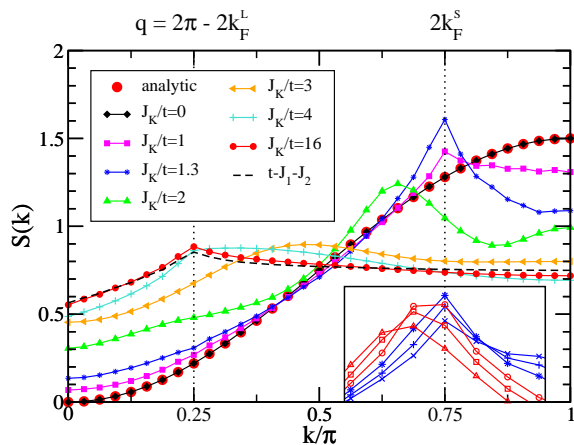


FIG. 4: (Color online) The magnetic structure factor of Eq. (5), plotted for $n = 0.75$ and the same values of J_K as in Fig. 3. For $J_K = 0$, the Kondo spins are locked in a perfect dimer state. The exact magnetic structure factor in this case (red dots) has a broad peak at $k = \pi$. Once J_K is switched on, a sharp cusp gradually develops at $2k_F^S = 0.75\pi$, reaching a maximum for $J_K/t \approx 1.3$. Upon further increasing J_K , the cusp smoothens and shifts continuously all the way to $q = 2\pi - 2k_F^L = 0.25\pi$, where a new cusp forms at large J_K . In the limit of large J_K , represented by $J_K/t = 16$, $S(k)$ well matches the structure factor of the corresponding $t - J_1 - J_2$ model, which is shown for comparison by the black dashed line. Inset: Evolution of the cusp at $2k_F^S$ as it first begins to move. Here crosses, pluses, stars, circles, squares, and triangles correspond to $J_K/t = 1.1, 1.2, 1.3, 1.4, 1.5$, and 1.6 , respectively. For $J_K/t \leq 1.3$ (blue lines), the cusp is pinned to $2k_F^S$, growing in magnitude with increasing J_K . For $1.4 \leq J_K/t$ (red lines), the cusp is shifted to incommensurate modulations.

action of the presumably frustrated spins on the conduction electrons.

D. Magnetic structure factor

The structure that $n(k)$ develops at k^* in the intermediate phase is rather small. We now show that a much more pronounced feature is found at $2k^*$ in the magnetic structure factor of the Kondo spins, defined as

$$S(k) = \sum_{i=1}^L \langle \vec{S}_i \cdot \vec{S}_{L/2} \rangle \cos[k(i - L/2)]. \quad (5)$$

Similar to $n(k)$, Eq. (5) is defined to match the OBC used. It reduces in the thermodynamic limit and in the absence of translational symmetry breaking to the Fourier transform of the spin-spin correlation function $\langle \vec{S}_i \cdot \vec{S}_j \rangle$.

Figure 4 shows the evolution of $S(k)$ with increasing J_K . For $J_K = 0$, when the spin chain locks in a perfect dimerized ground state, $S(k)$ equals $0.75[1 - \cos(k)]$. This curve, depicted by the red dots in Fig. 4, has a maximum

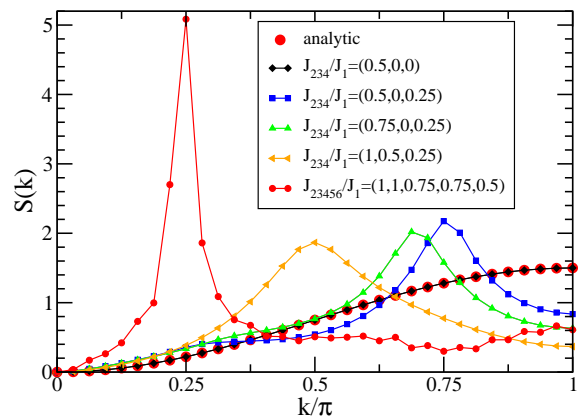


FIG. 5: (Color online) The magnetic structure factor of the effective Heisenberg Hamiltonian with different spin-exchange couplings J_1, J_2, \dots, J_6 , up to a distance of 6 lattice sites. Starting from the Majumdar-Ghosh point and gradually increasing the relative strengths of J_2 to J_6 , we are able to shift the main modulation in $S(k)$ from $k = \pi$ to $2k_F^S = 0.75\pi$, and then all the way to $q = 0.25\pi$, in close analogy to the peak positions observed in Fig. 4. The incommensurate modulations that are seen in Fig. 4 can thus be understood as due to the frustrated RKKY interaction, whose magnitude increases with J_K .

at $k = \pi$ and is well reproduced by our DMRG data. In the opposite limit of a large J_K , $S(k)$ reduces to the magnetic structure factor of the $t - J_1 - J_2$ model, which has a cusp at $q = 2\pi - 2k_F^L = \pi(1 - n) = 0.25\pi$ [note that q and $2k_F^L$ are equivalent by virtue of $S(k) = S(2\pi - k)$, and will be regarded as synonymous hereafter]. The transition between these two limits proceeds as follows.

When J_K is switched on, the spins couple to the conduction electrons. As a result, $S(k)$ gradually deforms from its perfect dimerized profile and develops a sharp cusp at $2k_F^S = 0.75\pi$, as can be seen for $J_K/t = 1$ and 1.3 . The evolution of this cusp is tracked in the inset. With increasing J_K the cusp initially grows sharper, until reaching a maximum for $J_K/t \approx 1.3$. Upon further increasing J_K ($1.4 \leq J_K/t \leq 4$), the cusp smoothens and shifts continuously all the way to $q = 0.25\pi$. Interestingly, the cusp at $2k_F^S$ first begins to shift at the same value of J_K where the dimerized order parameter D acquires its sharpest slope. Furthermore, in the intermediate regime $1.4 \leq J_K/t \lesssim 4$, the associated peak in $S(k)$ occurs at $q^* = 2\pi - 2k^*$, where k^* is the position of the additional structure found in $n(k)$. Hence the two features are intimately related. Lastly we note that the local maximum that is seen at $k = \pi$ for $J_K/t = 2$ is a finite-size effect that decreases in magnitude with increasing system size. This is in contrast to the incommensurate peaks at q^* which depend only weakly on L .

In order to understand the origin of the incommensurate modulations in $S(k)$, we studied an effective spin Hamiltonian which comes to mimic the RKKY interactions present in the KLM. Specifically, we consider a frustrated Heisenberg model with different spin-exchange in-

interactions J_1, J_2, \dots, J_6 , up to a distance of 6 lattice sites. Such an effective Hamiltonian with adequate couplings is expected to properly describe the spin dynamics in the KLM up to moderately large values of J_K . This description must eventually break down for large J_K , when the conduction electrons and spins tightly bind to form localized singlets.

Figure 5 shows the magnetic structure factor $S(k)$ for the effective Heisenberg model. As can be seen, we are able to generate incommensurate modulations in $S(k)$ by varying the relative strengths of the different spin-exchange interactions. In particular, starting from the Majumdar-Ghosh point and gradually increasing the relative strengths of J_2 to J_6 , we are able to shift the main modulation from $k = \pi$ (perfect dimers) to $2k_F^S = 0.75\pi$, and then all the way to $q = 0.25\pi$. Note that the peak positions in Fig. 5 are quite similar to those in Fig. 4, though their profiles progressively deviate from those in Fig. 4 upon increasing the couplings. This is to be expected from the approach to strong coupling, where the KLM reduces to the $t - J_1 - J_2$ model. These results indicate that the effective RKKY interaction between the Kondo spins is responsible for the incommensurate modulations observed in Fig. 4.

E. Density correlations and charge structure factor

In order to further prove the spin origin of the feature that $n(k)$ displays at k^* , we proceed to show results on density correlations and the charge structure factor. Figure 6 depicts the smoothed Fourier transform of the local density $n_r(k)$, defined as

$$n_r(k) = \sum_{i=1}^L \left[\langle \hat{n}_i - n \rangle - \frac{I}{J} \right] W(i) \cos \left[k \left(\frac{L+1}{2} - i \right) \right]. \quad (6)$$

Here, $n = 0.75$ is the filling factor, \hat{n}_i equals $\sum_{\sigma} \hat{n}_{i,\sigma}$ with $\hat{n}_{i,\sigma} = c_{i,\sigma}^\dagger c_{i,\sigma}$, and $W(i)$ is a smooth windowing function introduced to avoid spurious edge effects.^{25,26} The additional term I/J with $I = \sum_{i=1}^L \langle n_i - n \rangle W(i)$ and $J = \sum_{i=1}^L W(i)$ comes to correct for the weighted average of \hat{n}_i , which slightly deviates from n . Its role is to remove an artificial feature near $k = 0$ introduced by $W(i)$.

The Fourier transform of the local density oscillations is a measure of the Friedel oscillations that develop due to the OBC used. It thus offers a direct way to probe the Fermi momentum, which is manifest as a peak at $2k_F$ and its higher harmonics.^{25,26} Figure 6 shows the Friedel oscillations for three values of $J_K/t = 0, 1.3$ and 16 . For $J_K = 0$ we observe a single peak at $2k_F^S = 0.75\pi$, which well agrees with an exact evaluation of Eq. (6) using the single-particle eigen-modes of the decoupled conduction-electron chain (red circles). In the opposite limit of large J_K , there is one peak at $q = 2\pi - 2k_F^L = 0.25\pi$ and another peak at $2q = 0.5\pi$.²⁷ Both structures agree fa-

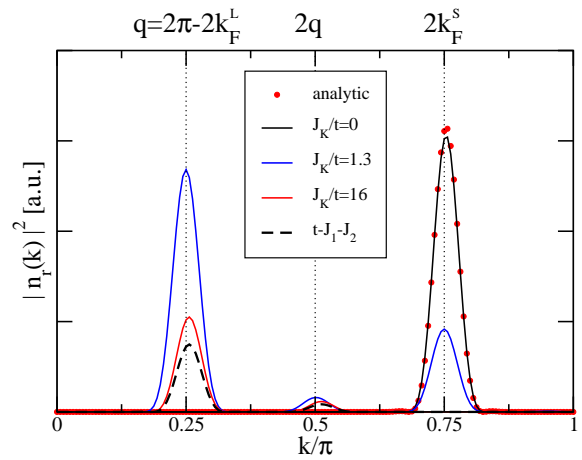


FIG. 6: (Color online) The smoothed Fourier transform of the local density defined in Eq. (6), for $n = 0.75$ and different Kondo interactions. For $J_K = 0$, there are pronounced Friedel oscillations at the modulation wavelength $2k_F^S = 0.75\pi$, in good agreement with an exact evaluation of Eq. (6) using the single-particle eigen-modes of the isolated tight-binding chain (red circles). At large J_K , represented by $J_K/t = 16$, there are Friedel oscillations at both $q = 2\pi - 2k_F^L = 0.25\pi$ and $2q = 0.5\pi$, in accordance with $|n_r(k)|^2$ for the corresponding $t - J_1 - J_2$ model (black dashed line). Surprisingly, for $J_K/t = 1.3$ there are simultaneous modulations at $2k_F^S$, q , and $2q$, as if there were two coexisting Fermi momenta k_F^S and k_F^L (note that $2q = 2\pi - 4k_F^S = 4\pi - 4k_F^L$ corresponds to both $4k_F^S$ and $4k_F^L$).

vorably with similar calculations for the corresponding $t - J_1 - J_2$ model,²⁸ whose results are shown by the black dashed line. Remarkably, for the intermediate coupling $J_K/t = 1.3$ we find modulations at all three momenta $2k_F^S$, q , and $2q$, as if there were two coexisting Fermi momenta²⁹ k_F^S and k_F^L (note that $2q$ corresponds both to $4k_F^S$ and $4k_F^L$). These results are in stark contrast to the electron momentum-distribution function of Fig. 3, which shows only a single step at k_F^S for this value of J_K .

As a function of J_K , the peak at $2k_F^S$ persists from $J_K = 0$ up to $J_K/t \approx 1.7$, which is the point where the dimerized order parameter $|D|$ first vanishes (see Fig. 1). Above $J_K/t \approx 1.7$ there are no discernable signatures left at $2k_F^S$. The peak at q appears continuously at small J_K , and persists all the way up to large J_K . It evolves, however, in a nonmonotonous fashion, first growing in magnitude before decreasing toward its asymptotic $t - J_1 - J_2$ -model form. Interestingly, no special signature appears at the incommensurate momentum $q^* = 2\pi - 2k^*$, indicating that k^* is unrelated to the FS.

Finally, in Fig. 7 we show the Fourier transform of the conduction-electron density-density correlation function, defined as

$$C(k) = \sum_{i=1}^L \langle (n_i - n)(n_{L/2} - n) \rangle \cos[k(i - L/2)]. \quad (7)$$

Similar to previous plots, the DMRG data well repro-

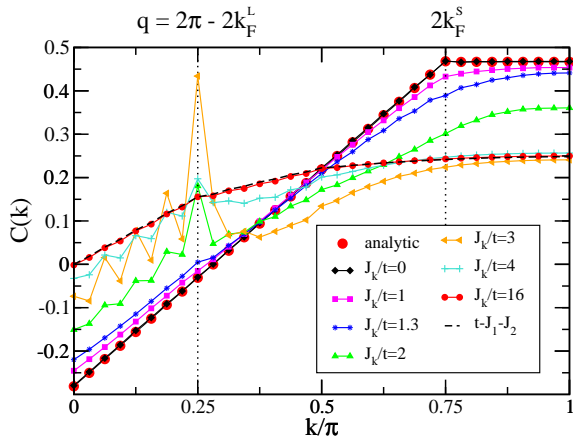


FIG. 7: (Color online) Fourier transform of the density-density correlation function of Eq. (7), for $n = 0.75$ and different Kondo interactions. For $J_K = 0$ there is a single sharp cusp at $2k_F^S = 0.75\pi$, in good agreement with the exact non-interacting result depicted by the red circles. For large J_K , the sharp structure at $2k_F^S$ is replaced with two very shallow cusps at $q = 2\pi - 2k_F^L = 0.25\pi$ and $2q$, in agreement with $C(k)$ for the corresponding $t - J_1 - J_2$ model²⁸ (black dashed line). At the intermediate couplings $J_K/t = 2, 3$, and 4 there is a sharp modulation at q , which degenerates into the shallow cusp of the $t - J_1 - J_2$ model upon increasing J_K .

duce the exact noninteracting result for $J_K = 0$, and are consistent with the $t - J_1 - J_2$ model for large J_K . For $J_K = 0$ there is a single sharp cusp at $2k_F^S = 0.75\pi$, which gradually smoothens as J_K is switched on. For large J_K (represented by $J_K/t = 16$), there are two very shallow cusps at q and $2q$, corresponding to modulations at $2k_F^L$ and $4k_F^L$. Both limits of small and large J_K are compatible with the Friedel oscillations observed in Fig. 6.

A more complex structure is found for the intermediate couplings $J_K/t = 2, 3$ and 4 . Here a sharp modulation develops at q , accompanied by additional wiggles at smaller values of k . We believe that the latter wiggles are a finite-size effect since they can be practically removed by using a windowing function that smoothly falls off toward the chain edges. By contrast, the primary peak at q not only persists but actually grows in magnitude if a windowing function is used. Similar to the Friedel oscillations, the primary peak at q evolves nonmonotonically with increasing J_K , first growing in magnitude before degenerating into the shallow cusp of the $t - J_1 - J_2$ model for large J_K . The overall behavior of $C(k)$ in this regime is consistent with a tendency toward charge-density-wave or superconducting correlations that may accompany the opening of a spin gap. Lastly we note that $C(k)$ shows no discernable signature related to k^* , reinforcing the spin origin of this modulation wavelength.

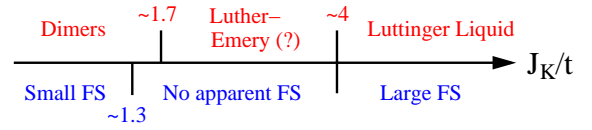


FIG. 8: (Color online) Phase diagram of the KLM of Eq. (1), for $J_{H_1} = 2J_{H_2} = t/2$ and $n = 0.75$. At weak coupling, $0 \leq J_K/t \lesssim 1.3$, the system is in a gapless dimer state with the small Fermi momentum $k_F^S = \pi n/2$. A spin-gapped phase sets in at intermediate coupling $1.3 \lesssim J_K/t \lesssim 4$, part of which retains nonzero dimer order (for $1.3 \lesssim J_K/t \lesssim 1.7$) and part of which where no dimer order is left (for $1.7 \lesssim J_K/t \lesssim 4$). The spin-gapped phase lacks a clear Fermi momentum. Finally, for $4 \lesssim J_K/t$ the system enters a paramagnetic LL phase with $k_F^L = \pi(n+1)/2$ serving as the new Fermi momentum.

IV. DISCUSSION AND CONCLUSIONS

We begin by summarizing the zero-temperature phase diagram of the KLM of Eq. (1), for $J_{H_1} = 2J_{H_2} = t/2$ and $n = 0.75$. For weak Kondo couplings, $0 \leq J_K/t \lesssim 1.3$, the system is in a gapless dimer state with the small Fermi momentum $k_F^S = \pi n/2 = 0.375\pi$. At intermediate Kondo couplings, $1.3 \lesssim J_K/t \lesssim 4$, a spin-gapped phase sets in,²⁴ part of which retains nonzero dimer order $|D|$ (for $1.3 \lesssim J_K/t \lesssim 1.7$), and part of which where no dimer order is left (for $1.7 \lesssim J_K/t \lesssim 4$). In the latter regime the system is presumably a Luther-Emery liquid. In contrast to the dimer state at weak coupling, the spin-gapped phase lacks a clear FS. There is no distinctive step in the electron momentum-distribution function, and the magnetic structure factor for the Kondo spins displays incommensurate modulations at $2k^*$, where k^* is a new characteristic momentum. The latter wavelength is not associated with a new Fermi momentum, as neither the Friedel oscillations encoded in $n_r(k)$ nor the density-density correlation function $C(k)$ show any discernable signatures related to k^* . Rather, above $J_K/t \approx 1.7$ both $n_r(k)$ and $C(k)$ display pronounced modulations related to k_F^L alone, in contrast to the regime $J_K/t \lesssim 1.7$ where $n_r(k)$ has simultaneous modulations at $2k_F^S$ and $2k_F^L$. Finally, for $4 \lesssim J_K/t$ the system enters the paramagnetic LL phase of the effective $t - J_1 - J_2$ model, with k_F^L serving as the new Fermi momentum. A sketch of the resulting phase diagram of the KLM is displayed in Fig. 8.

It should be emphasized that the opening of a spin gap in the KLM is by itself not new. A spin-gapped phase has long been established⁹ for the Kondo-Heisenberg model with $n < 1$ and $J_{H_2} = 0$, including recent indications for quasi-long-range superconducting correlations at a nonzero momentum.³⁰ Here, however, the spin-gapped phase shows up as an intermediate phase, separating two paramagnetic phases with different Fermi momenta. This is quite different from previous results for $J_{H_2} = 0$,⁹ where a single gapless phase was reported for values of J_K that exceeded the spin-gapped phase.

Our results should be compared to those of Pivovarov and Si,¹⁵ who used a perturbative renormalization-group

(RG) analysis to study a more general form of the KLM, including the effect of spin-exchange anisotropy in J_{H_1} and J_{H_2} . For the SU(2) spin-symmetric interactions considered here, the perturbative RG and DMRG results differ in two respects: (i) Perturbative RG predicts a region of coexistence between the weak-coupling spin-Peierls phase and the strong-coupling Kondo-singlet phase, whereas no such region is found by the DMRG. (ii) The strong-coupling phase is predicted by RG to have a spin gap, while our DMRG study finds a LL. Indeed, we have verified by explicit calculations that the $t - J_1 - J_2$ Hamiltonian onto which the system maps at strong coupling is gapless for $n_{\text{hole}} = 0.75$, thus forming a LL. Note, however, that a spin-gapped phase is expected in the $t - J_1 - J_2$ model as well when tuned sufficiently close to half filling (i.e., for $n \ll 1$ in the KLM).

The transition studied in this work does not appear to be consistent with the local picture for the QPT in heavy fermion compounds.^{13,14} We did not observe a sudden change in the size of the FS, despite the fact that such a change would be more favorable in 1D where the FS is reduced to just two isolated points. The intermediate spin-gapped phase for $1.3 \lesssim J_K/t \lesssim 4$ seems to be a region where the Fermi surface reconstructs from k_F^S to k_F^L .

It is not obvious to what extent can the QPT studied in this work be compared to transitions involving true magnetic order, as seen experimentally in heavy fermions systems. For instance, the opening of a spin gap in the intermediate phase appears to be related to our choice of the Majumdar-Ghosh ground state for the isolated spin chain. Nevertheless, frustration can arise directly from the RKKY interaction itself, as is known to occur at quarter filling.¹⁸ We have studied the Hamiltonian of Eq. (1) for $n = 0.5$ both with and without explicit frustration and found the same qualitative behavior. The electron momentum-distribution function $n(k)$ displayed the same general behavior as for $n = 0.75$, including an intermediate region with no apparent Fermi momentum. At the same time, we did not find any spin gap in the intermediate regime, nor did we identify any new characteristic momentum k^* associated with a shifting

structure in either $n(k)$ or $S(k)$. The absence of k^* for $n = 0.5$ likely stems from the fact that $2k_F^S$ and $2k_F^L$ are indistinguishable for this particular filling factor.

This naturally raises the question of how generic is the transition observed for $n = 0.75$. Is it representative of other filling factors in Eq. (1) or does the QPT vary qualitatively as a function of n ? Preliminary results for $n = 0.25$ and $n = 0.875$ suggest the following.³¹ For all filling factors studied there is an intermediate region where k_F cannot be defined. This aspect, as well as the overall behavior of the momentum-distribution function, appears to be generic. However, details of the intermediate region do depend on n . As stated above, we did not find any spin gap for $n = 0.5$, in contrast to the filling factors $n = 0.75$ and 0.875 which are both spin gapped and in qualitative agreement with each other. The picture for $n = 0.25$ seems to be more complex, and may potentially involve more than one intermediate phase. This possibility, currently under study, may suggest a qualitative difference between the regimes $n < 0.5$ and $0.5 < n < 1$.

To conclude, we conducted an exhaustive investigation of the transition from a spin-Peierls phase with a small Fermi momentum to a LL phase with a large Fermi momentum in a 1D KLM. Our findings indicate a rather complex transition that exceeds the predictions of local criticality. It remains to be seen which of our results extend to other electronic fillings and other variants of the 1D KLM, let alone to higher dimensions. Further investigations of this fascinating issue are clearly in order.

Acknowledgments

We are grateful to Dror Orgad and Efrat Shimshoni for illuminating discussions. We are particularly thankful to Efrat Shimshoni for stimulating our interest in this problem. This work was supported in part by a Shapira fellowship of the Israeli Ministry of Immigrant Absorption (S.M.), and by the Israel Science Foundation through grant no. 1524/07.

¹ S. Doniach, *Physica B* **91**, 231 (1977).

² A. C. Hewson, *The Kondo Problem to Heavy Fermions* (Cambridge University Press, Cambridge, 1993).

³ M. Oshikawa, *Phys. Rev. Lett.* **84**, 3370 (2000).

⁴ J. M. Luttinger, *Phys. Rev.* **119**, 1153 (1960).

⁵ H. Tsunetsugu, M. Sigrist, and K. Ueda, *Rev. Mod. Phys.* **69**, 809 (1997).

⁶ N. Shibata, K. Ueda, T. Nishino, and C. Ishii, *Phys. Rev. B* **54**, 13495 (1996).

⁷ N. Shibata, A. Tsvetlik, and K. Ueda, *Phys. Rev. B* **56**, 330 (1997).

⁸ S. Moukouri and L. G. Caron, *Phys. Rev. B* **54**, 12212 (1996).

⁹ A. E. Sikkema, I. Affleck, and S. R. White, *Phys. Rev.*

Lett. **79**, 929 (1997).

¹⁰ M. Yamanaka, M. Oshikawa, and I. Affleck, *Phys. Rev. Lett.* **79**, 1110 (1997).

¹¹ J. C. Xavier, E. Novais, and E. Miranda, *Phys. Rev. B* **65**, 214406 (2002).

¹² M. Gulàcsi, *Adv. Phys.* **53**, 769 (2004).

¹³ P. Coleman, C. Pépin, Q. Si, and R. Ramazashvili, *J. Phys.: Condens. Matter* **13**, R723 (2001).

¹⁴ Q. Si, J-X. Zhu, and D. R. Grempel, *J. Phys.: Condens. Matter* **17** R1025 (2005).

¹⁵ E. Pivovarov and Q. Si, *Phys. Rev. B* **69**, 115104 (2004).

¹⁶ C. K. Majumdar and D. Ghosh, *J. Math. Phys.* **10**, 1388 (1969); C. K. Majumdar, *J. Phys. C: Solid State Phys.* **3** 911 (1969).

- ¹⁷ S. R. White, Phys. Rev. Lett. **69**, 2863 (1992); Phys. Rev. B **48**, 10345 (1993).
- ¹⁸ J. C. Xavier, R. G. Pereira, E. Miranda, and I. Affleck, Phys. Rev. Lett. **90**, 247204 (2003).
- ¹⁹ N. Shibata and C. Hotta, arXiv:cond-mat/0503476 (unpublished); C. Hotta and N. Shibata, Physica B **378-380**, 1039 (2006).
- ²⁰ J. C. Xavier and E. Miranda, Phys. Rev. B **78**, 144406 (2008).
- ²¹ An infinite system possesses two degenerate ground states, each displaced by one lattice site with respect to the other, and a finite energy gap to the first excitation energy. This ground-state degeneracy is lifted for a finite system with OBC, yet is quickly restored as $L \rightarrow \infty$. In contrast, the energy gap to the second excited state saturates at a nonzero constant as $L \rightarrow \infty$.
- ²² We use the prevailing convention whereby the hole filling factor is measured with respect to a half-filled band. In other words, n_{hole} measures the fraction of empty sites in the $t - J_1 - J_2$ model.
- ²³ The data displayed in Fig. 2 was obtained keeping 512 states in each of the external blocks. Only a small variation of order 1% was found in $\Delta_s(L \rightarrow \infty)$ for $J_K/t = 2.5$ when 256 states were kept.
- ²⁴ As can be seen in Fig. 2, there is no spin gap for $J_K/t = 4$. Indeed, as a function of J_K the gap appears to close somewhere between $J_K/t = 3$ and $J_K/t = 4$, which defines the location of the upper phase boundary. The position of the lower phase boundary is harder to pinpoint. We estimate it to lie close to $J_K/t = 1.3$, where both the dimer order parameter $|D|$ and the spin velocity v_s show significant changes in behavior.
- ²⁵ S. R. White, I. Affleck, and D. J. Scalapino, Phys. Rev. B **65**, 165122 (2002).
- ²⁶ M. Vekic and S. R. White, Phys. Rev. Lett. **71**, 4283 (1993); We used the same windowing function as described in Eqs. (4) and (10) of this paper.
- ²⁷ Due to the introduction of a windowing function, there is a slight shift in the positions of the peaks away from q and $2q$. We have confirmed that these shifts depend on the choice of $W(i)$ and are not inherent to the model.
- ²⁸ Strictly speaking, the mapping onto the $t - J_1 - J_2$ model requires that $n_r(k)$ and $C(k)$ be computed using the local hole (i.e., empty-site) densities rather than the electronic densities. However, $|n_r(k)|$ and $C(k)$ are identical for holes and electrons in the $t - J_1 - J_2$ model due to the omission of doubly occupied states.
- ²⁹ Note that the peak at 0.25π can also be interpreted as corresponding to $6k_F^S$. Nevertheless, we find such a pronounced modulation at $6k_F$ to be highly unlikely.
- ³⁰ E. Berg, E. Fradkin, and S. A. Kivelson, Phys. Rev. Lett. **105**, 146403 (2010).
- ³¹ Since $0 < n < 1$ and $1 < n < 2$ are related by particle-hole symmetry, it suffices to consider $0 < n < 1$.